Cement and Concrete Research 40 (2010) 167–170

Contents lists available at ScienceDirect

Cement and Concrete Research

journal homepage: http://ees.elsevier.com/CEMCON/default.asp

Melt differentiation and crystallization of clinker minerals in a $CaO–SiO_2–Al_2O_3–Fe_2O_3$ pseudoquaternary system

Koichiro Fukuda [a,*], Tomoyuki Iwata [a], Hideto Yoshida [b]

[a] Department of Materials Science and Engineering, Nagoya Institute of Technology, Nagoya 466-8555, Japan
[b] Department of Earth and Planetary Science, Graduate School of Science, The University of Tokyo, Tokyo 113-0033, Japan

ARTICLE INFO

Article history:
Received 2 February 2009
Accepted 21 August 2009

Keywords:
Microstructure (B)
Clinker (D)
Portland Cement (D)
Calcium aluminoferrite (D)
Melt differentiation

ABSTRACT

In the $CaO–SiO_2–Al_2O_3–Fe_2O_3$ pseudoquaternary system, the solid solutions of Ca_3SiO_5 [C_3S(ss)], Ca_2SiO_4 [C_2S(ss)], $Ca_2(Al_xFe_{1-x})_2O_5$ with $0.40 \le x \le 0.57$ (ferrite) and $Ca_3Al_2O_6$ [C_3A(ss)] were crystallized out of a complete melt with 52.9 mass% CaO and $Al_2O_3/Fe_2O_3 = 0.70$. When the melt was cooled from 1673 K at 80 K/h, the crystals of ferrite with $x = 0.40$, C_3S(ss) and C_2S(ss) would start to nucleate from the melt at 1630 K. During further cooling, the x value of the precipitating ferrite would progressively increase and eventually approach 0.57 at 1613 K. The resulting ferrite crystals showed a zonal structure, the x value of which successively increased from the cores toward the rims. Actually, the x values of 0.43 and 0.52 were confirmed for, respectively, the cores and rims by EPMA. As the simultaneous crystallization of zoned ferrite, C_3S(ss) and C_2S(ss) proceeded, the coexisting melt would become progressively enriched in the Al_2O_3 component. After the termination of the ferrite crystallization, the C_3A(ss), C_3S(ss) and C_2S(ss) crystallized out of the differentiated melt. The end result was the four phase mixture of ferrite, C_3A(ss), C_3S(ss) and C_2S(ss), being free from the nucleation of $Ca_{12}Al_{14}O_{33}$ solid solution.

1. Introduction

Phase stabilities in parts of the P_2O_5-bearing pseudoquaternary $CaO–SiO_2–Al_2O_3–Fe_2O_3$ system have been investigated by isothermal heating experiments over the temperature range of 1873–1573 K [1–3]. On the basis of chemical compositions of coexisting phases at constant temperatures, a melt-differentiation reaction has been proposed to occur during cooling, which satisfactory accounts for the formation mechanism of chemical zoning in $Ca_2(Al_xFe_{1-x})_2O_5$ (ferrite, $0 \le x \le 0.7$) [4,5] as well as the crystallization behaviors of the solid solutions $Ca_3Al_2O_6$ [C_3A(ss)] and $Ca_{12}Al_{14}O_{33}$ [$C_{12}A_7$(ss)]. The predicted differentiation paths have been different between the two types of melts with the CaO concentrations of 51–54 mass% and the lower [3]. When the former melt underwent differentiation by the crystallization of Ca_3SiO_5 solid solution [C_3S(ss)], Ca_2SiO_4 solid solution [C_2S(ss)] and ferrite during cooling from 1663 to 1613 K, the Al_2O_3/Fe_2O_3 value of the melt ($= AR_m$) has been expected to steadily increase from 0.25 to 1.74 [3]. Upon subsequent cooling, the C_3A(ss) would start to crystallize out of the differentiated melt at ~1584 K. The resulting phase composition at ambient temperature has been therefore C_3S(ss), C_2S(ss), ferrite and C_3A(ss). On the other hand, not only C_3A(ss) but also $C_{12}A_7$(ss) have been expected to eventually crystallize when the C_3S(ss)-free melts having the lower CaO concentration of 47–51 mass% ($0.25 \le AR_m \le 2.6$) differentiated by the crystallization of C_2S(ss) and ferrite [2]. The phase composition at ambient temperature has been expected to be C_2S(ss), ferrite, C_3A(ss) and $C_{12}A_7$(ss), because the chemical composition of the finally differentiated melt, the AR_m-value of which was around 4.5 at 1583 K, would lie within the C_2S(ss)-ferrite($x = 0.7$)–C_3A(ss)–$C_{12}A_7$(ss) subsystem. It should be noted that the predicted phase composition is free from C_3S(ss).

For the complete melt with the particular CaO concentration of 50.0 mass% ($AR_m = 0.70$), the slow cooling experiment has been conducted in the temperature range from 1773 to 1273 K [6]. As the crystallization of C_2S(ss) and zoned ferrite proceeded during cooling, the AR_m-value of melt successively increased, which resulted in the formation of both C_3A(ss) and $C_{12}A_7$(ss). In the present study, we have performed the similar crystallization experiment for the complete melt with the higher CaO concentration of 52.9 mass%. Provided the differentiation occurs according to the predicted path, the phase composition at ambient temperature should be C_3S(ss), C_2S(ss), ferrite and C_3A(ss), without the crystallization of $C_{12}A_7$(ss) being initiated.

2. Experimental

2.1. Materials

In a previous study [3], the crystals of C_3S(ss), C_2S(ss) and ferrite with $Al/(Al + Fe) = 0.40$ coexisted in equilibrium with a melt (52.9 mass % CaO and $AR_m = 0.70$) at 1630 K. The bulk chemical composition of the present specimen was identical to that of this particular melt (Fig. 1).

* Corresponding author.
E-mail address: fukuda.koichiro@nitech.ac.jp (K. Fukuda).

0008-8846/$ – see front matter © 2009 Elsevier Ltd. All rights reserved.
doi:10.1016/j.cemconres.2009.08.016

The appropriate amounts of reagent-grade chemicals (Table 1) were well mixed and pressed into pellets (12 mm diameter and 3 mm thick). They were heated to 1673 K at 500 K/h, completely melted for 1 h, cooled to 1273 K at 80 K/h, then quenched in air. During the slow cooling process, the ferrite crystals developed, in the presence of melt, together with much smaller amounts of C_3S(ss), C_2S(ss) and C_3A(ss) crystals. A small amount of P_2O_5 was added to suppress the β-to-γ phase transition of C_2S(ss) during quenching and prevent the disintegration of the crystals.

2.2. Characterization

A polished thin section was prepared and the microtexture was observed with both transmitted and reflected light. The concentration distribution maps for Al_2O_3, Fe_2O_3, CaO, SiO_2 and P_2O_5 were obtained using an electron probe microanalyzer (EPMA, Model JXA-8900L, JEOL, Ltd., Tokyo, Japan). The area of analysis on the sample was 250 μm × 450 μm with 500 × 900 pixels and the dwell time was 15 ms. The accelerating voltage was 15 kV, the probe current was 0.012 μA and the electron probe diameter was ~1 μm. Quantitative spot analyses were made within the same area. The corrections were made by ZAF routines.

The phase composition was examined by X-ray powder diffractometry (XRPD) in order to confirm the absence of $C_{12}A_7$(ss). The XRPD intensities were collected on a diffractometer (X'Pert PRO Alpha-1, PANalytical B.V., Almelo, the Netherlands) equipped with a high-speed detector in Bragg–Brentano geometry using monochromatized CuKα$_1$ radiation (45 kV, 40 mA) in a 2θ range from 10° to 80°. Peak positions of the experimental diffraction pattern were determined by finding minimums in the second derivatives using the computer program PowderX [7].

3. Results and discussion

3.1. Compositional variation of constituent phases

The XRPD pattern showed that the sample was composed exclusively of ferrite, C_3A(ss), C_3S(ss) and C_2S(ss), without the crystallization of $C_{12}A_7$(ss) being initiated. The lath-shaped ferrite phenocrysts in Fig. 2 showed, in transmitted light, a zonal structure with a color varying from dark brown at the cores to yellowish pale brown toward the rims. The chemical zoning was confirmed by the concentration distribution maps for Al_2O_3 and Fe_2O_3 (Fig. 3). The

Table 1
Preparation of raw mixture.

Reagent	Bulk composition (mass%)
SiO_2	4.38
Fe_2O_3	16.99
Al_2O_3	11.89
$CaHPO_4 \cdot 2H_2O$	0.12
$CaCO_3$	66.62
Total	100
Substance	**Bulk composition (mass%)[a]**
SiO_2	6.20
Fe_2O_3	24.04
Al_2O_3	16.83
P_2O_5	0.07
CaO	52.86
Total	100
SiO_2*	6.26
	Mass ratio
Al_2O_3/Fe_2O_3	0.70
	Atomic ratio
Al/Fe	1.10
Al/(Al + Fe)	0.52

The amounts of P_2O_5 are added to those of SiO_2 as $0.847P_2O_5$; the total [$SiO_2 + 0.847P_2O_5$] is denoted by SiO_2*.
[a] Re-calculated for non-volatile components.

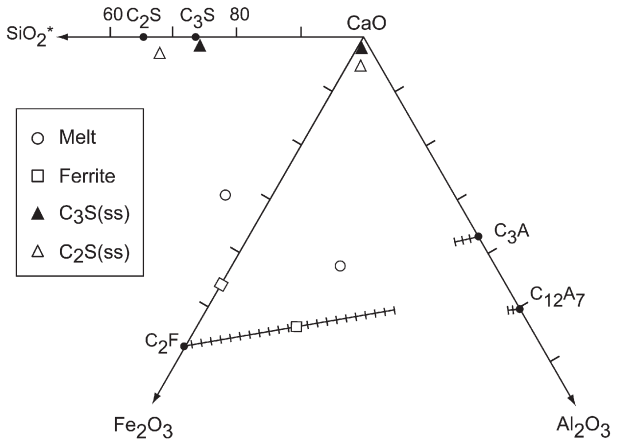

Fig. 1. Compositions of melt, ferrite with Al/(Al + Fe) = 0.40, C_3S(ss) and C_2S(ss) on portions of the quaternary system CaO–Al_2O_3–Fe_2O_3–SiO_2^* [3]. These four phases coexist in equilibrium at 1630 K. The amounts of P_2O_5 are added to those of SiO_2 as $0.847P_2O_5$ and the total [$SiO_2 + 0.847P_2O_5$] is denoted by SiO_2^*. Hatched lines indicate solid solutions in the formulae $Ca_2(Al_xFe_{1-x})_2O_5$ with x between 0 and 0.7, $Ca_3(Al_{1-y}Fe_y)_2O_6$ with y between 0 and 0.04, and $Ca_{12}(Al_{1-z}Fe_z)_{14}O_{33}$ with z between 0 and 0.03 [6].

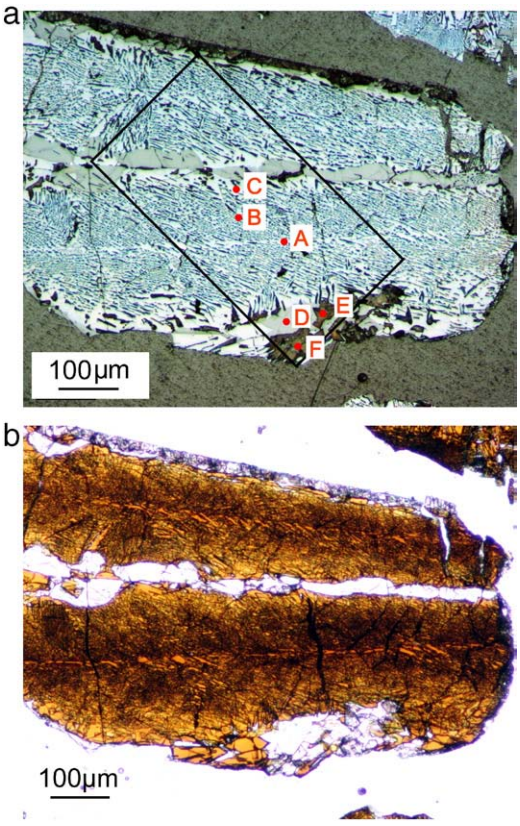

Fig. 2. Optical micrograph of lath-shaped ferrite phenocrysts and much smaller crystals of C_3S(ss), C_2S(ss) and C_3A(ss). Polished thin section etched with nital. (a) Reflected light and (b) transmitted light. The zonal structure from the cores toward the rims is clearly recognized for the ferrite phenocrysts by the change in color from dark brown to yellowish pale brown in (b). Red closed circles mark the locations of the electron probe microanalyses referred to in the text.

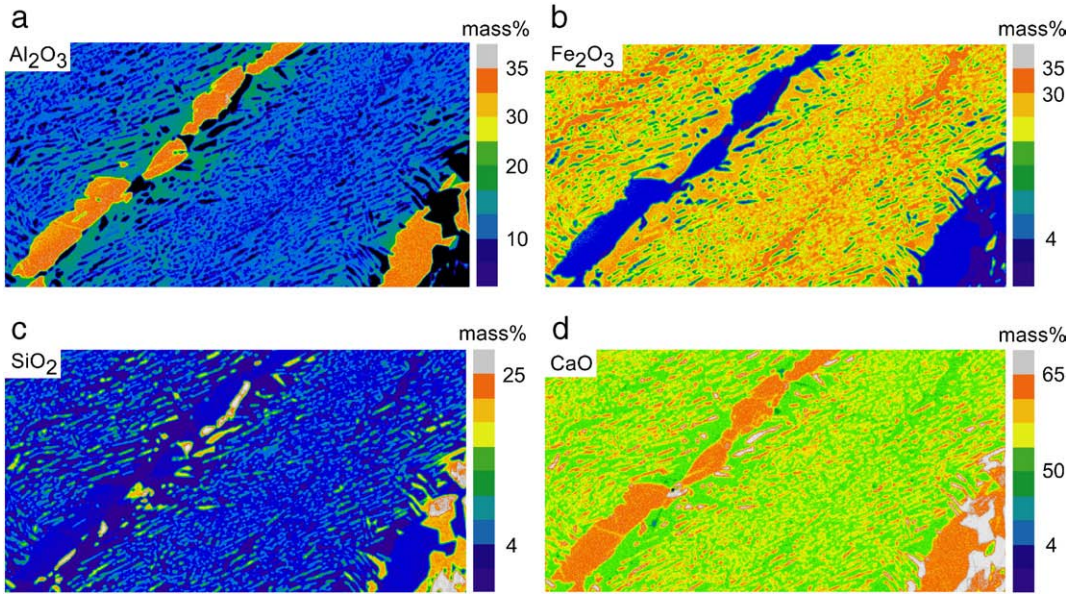

Fig. 3. Concentration distribution maps for (a) Al_2O_3, (b) Fe_2O_3, (c) SiO_2 and (d) CaO in the area depicted by the open square in Fig. 2a. The figures beside the color columns represent the mass percentage of the relevant oxides.

cores were richer in Fe_2O_3 than the rims, while the concentration of Al_2O_3 was inversely distributed, in agreement with previous studies [4,5]. These two maps as well as the quantitative spot analyses at points A, B and C in Fig. 4 reveal that the Al/Fe ratio gradually increased from the core to the rim (Table 2). The crystallization was accompanied by the intergrowth of minute (<1 μm) crystals of C_3S(ss) and C_2S(ss) (Fig. 2a). This implies that the chemical compositions determined at those points are mainly of ferrite with small amounts of C_3S(ss) and C_2S(ss), however the chemical data almost lie on the hatched line indicating ferrite solid solution on the CaO–Al_2O_3–Fe_2O_3–SiO_2 quaternary diagram (Fig. 4). Accordingly, the x values of the ferrite would be 0.43 at point A, 0.48 at point B and 0.52 at point C (Table 2), indicating that the zonal structure of the ferrite phenocryst was characterized by the progressive increase in the x value from 0.43 at the cores to 0.52 at the rims. The chemical zoning confirmed in the present study is substantially identical to that predicted in a previous study [3]. The unit-cell dimensions of the zoned ferrite were determined from the XRPD data to be $a=0.55685(8)$ nm, $b=1.4521(2)$ nm, $c=0.53697(7)$ nm and $V=0.4342(1)$ nm^3, which were found from the 2θ values with reflection indices of 020, 130, 200, 002 and 141. Because the cell dimensions of ferrite steadily decrease with increasing Al/(Al + Fe) ratio [8], the above cell dimensions would correspond to those of the homogeneous ferrite, the chemical composition of which is identical with that of the averaged of the zoned ferrite.

Between the ferrite phenocrysts, viewed under reflected light, dark gray regions occur consisting of C_3A(ss) crystals (Fig. 2a). They were necessarily adjacent to the ferrite rims with sharp interface boundaries. The composition at point D in Fig. 2a was representative of C_3A(ss), the chemical formula of which is $Ca_{2.94}[Al_{1.77}Fe_{0.14}Si_{0.10}]_{\Sigma 2.01}O_6$ with the Al/(Al + Fe) value being 0.92 (Table 2). The C_3A(ss) accommodated about 4.2 mass% Fe_2O_3 and 2.1 mass% SiO_2, while the other oxide P_2O_5 was not detectable (Table 2). The crystal system must be cubic because the phase composition is almost independent of incorporation of Fe_2O_3 and/or

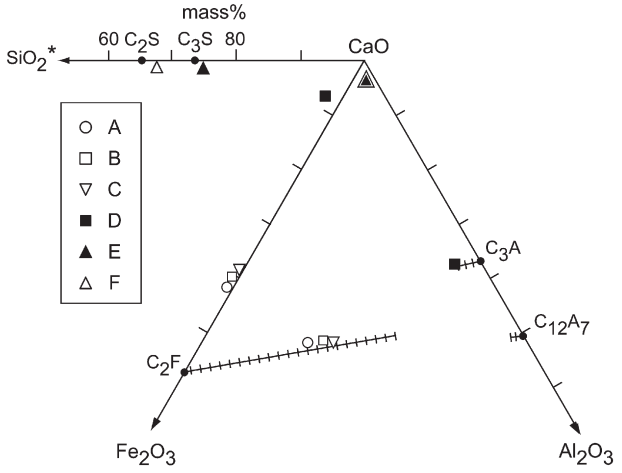

Fig. 4. Analytical data for sampling points A–F in Fig. 2a and Table 2. Compositions are plotted on portions of the quaternary system CaO–Al_2O_3–Fe_2O_3–SiO_2^*. The hatched lines indicate solid solutions. The amounts of P_2O_5 are added to those of SiO_2 as $0.847P_2O_5$ and the total [$SiO_2 + 0.847P_2O_5$] is denoted by SiO_2^*.

Table 2
Chemical compositions determined at sampling points A–F in Fig. 2a.

Substance	Chemical composition (mass%)[a]					
	Point A	Point B	Point C	Point D	Point E	Point F
SiO_2	1.14	0.91	0.47	2.14	24.68	31.57
Fe_2O_3	35.16	32.74	30.92	4.24	1.23	1.10
Al_2O_3	17.10	19.44	21.20	33.05	1.47	1.32
P_2O_5	ND	ND	ND	ND	0.71	1.43
CaO	46.58	46.90	47.39	60.56	71.91	64.58
Total	100	100	100	100	100	100
SiO_2*	1.16	0.92	0.48	2.15	25.28	32.78
	Number of atoms					
Ca	2.043	2.036	2.043	2.941	2.921	1.992
Fe	–	–	–	–	0.035	–
Σ	2.043	2.036	2.043	2.941	2.956	1.992
Si	0.047	0.037	0.019	0.097	0.935	0.909
Al	0.825	0.928	1.006	1.765	0.066	0.045
Fe	1.083	0.998	0.937	0.144	–	0.024
P	–	–	–	–	0.023	0.034
Σ	1.955	1.963	1.962	2.007	1.024	1.012
O	5	5	5	6	5	4
Al/(Al + Fe)	0.432	0.482	0.518	0.924	0.651	0.652
Main phase	Ferrite	Ferrite	Ferrite	C_3A(ss)	C_3S(ss)	C_2S(ss)

ND is not detectable.
The amounts of P_2O_5 are added to those of SiO_2 as $0.847P_2O_5$; the total [$SiO_2 + 0.847P_2O_5$] is denoted by SiO_2*.
[a] Total is normalized to be 100 mass%.

SiO_2 [9,10]. Actually the cubic cell dimension was successfully determined from the XRPD data to be 1.52740(8) nm and $V = 3.5633$ (6) nm^3 based on the 2θ values with reflection indices of 440, 800 and 844. The quantitative chemical data consistently lies, when plotted as mass ratios on the $CaO–Al_2O_3–Fe_2O_3$ ternary diagram (Fig. 4), on the hatched line indicating the solid solution. The distribution of C_3A(ss) was clearly demonstrated by the >30 mass% area in the distribution map for Al_2O_3 (Fig. 3a). The presence of $C_{12}A_7$(ss), which should be composed of ~50 mass% Al_2O_3, was not confirmed by the Al_2O_3 distribution map, in accordance with the XRPD result.

The C_3S(ss) and C_2S(ss) crystals between the ferrite phenocrysts, for example at points respectively E and F in Fig. 2a, were much larger (up to 10 μm) than those that were co-crystallized with the phenocrysts. The chemical formulas were $[Ca_{2.92}Fe_{0.04}]_{\Sigma 2.96}[Si_{0.94}Al_{0.07}]_{\Sigma 1.01}O_5$ for the former crystal and $Ca_{1.99}[Si_{0.91}Al_{0.05}Fe_{0.02}P_{0.03}]_{\Sigma 1.01}O_4$ for the latter. Each distribution of the silicates was well shown by the SiO_2 map (Fig. 3c), because this component is present in higher concentration than 25 mass% for C_2S(ss) and vice versa for C_3S(ss). The P_2O_5 component showed a tendency to concentrate in C_3S(ss) and C_2S(ss) crystals. The concentrations were higher for C_2S(ss) than for C_3S(ss) as shown in Table 2. However, the extremely low concentration of P_2O_5 provided a low resolution for the distribution map, which was therefore omitted in the present paper.

3.2. Crystallization sequence during cooling

When the melt with 52.9 mass% CaO and $AR_m = 0.70$ was cooled from 1673 K, the ferrite, C_3S(ss) and C_2S(ss) would start to crystallize at around 1630 K according to the sequence of events as predicted in a previous study [3]. The x value of the initial ferrite is expected to be 0.40, because this value is of the particular ferrite that should be in equilibrium with the melt at 1630 K. Actually the comparable value of 0.43 was determined for the cores of the ferrite phenocrysts. During further cooling, the ferrite, C_3S(ss) and C_2S(ss) would continue to crystallize, with the x value of the former progressively increasing up to about 0.57. For the ferrite rims, the value of 0.52 was actually determined. At around 1613 K during cooling, the C_3A(ss) would start to crystallize out of the differentiated melt. The large-size crystals of C_3S(ss) and C_2S(ss) that were in contact with the ferrite rims were most probably formed below 1613 K. During subsequent cooling, equilibrium within the ferrite crystals is not attained, and hence the zonal structure is preserved to ambient temperature.

As the simultaneous precipitation of zoned ferrite, C_3S(ss) and C_2S(ss) proceeds, the coexisting melt would become progressively enriched in Al_2O_3 component; the AR_m-value of the melt would steadily increase from 0.70 to 1.74 during cooling from 1630 K to 1613 K. The crystallization of $C_{12}A_7$(ss) is hardly expected because the chemical composition of the finally differentiated melt would lie within the C_3S(ss)–C_2S(ss)–ferrite–C_3A(ss) subsystem [3]. Immediately after the termination of the crystallization of ferrite at around 1613 K, the three phases of C_3S(ss), C_2S(ss) and C_3A(ss) would start to precipitate out of the residual melt. Accordingly, the regions composed of these three phases were necessarily adjacent to the ferrite rims with sharp interface boundaries.

The presence of $C_{12}A_7$(ss) in production cement clinkers is one of the long-standing questions [10]. Lea (1935) have investigated the phase stability in the pure quaternary system $CaO–SiO_2–Al_2O_3–Fe_2O_3$ and found that the Al_2O_3/Fe_2O_3 value of cement clinkers ($= AR_s$) played an important role in the crystallization of C_3A(ss) and $C_{12}A_7$(ss) [11]. According to his results, the phase composition at ambient temperature would be C_3S(ss), C_2S(ss), ferrite and C_3A(ss) if the AR_s-value is between 0.7 and 1.7, whereas, if the AR_s-value exceeds 1.7, the $C_{12}A_7$(ss) would be formed at the expense of C_3A(ss). The threshold AR_s-value would be around 1.7, which corresponded to $AR_m = 2.0$ for the interstitial melt in cement clinkers [3]. In a previous study, the $C_{12}A_7$(ss) actually crystallized, together with C_2S(ss), C_3A(ss) and ferrite with $x = 0.7$, out of the melt with $AR_m = 4.0$ (51.9 mass% CaO) [3]. Because the chemical composition of this melt originally lies within the C_2S(ss)–ferrite($x = 0.7$)–C_3A(ss)–$C_{12}A_7$(ss) subsystem, the crystallization of $C_{12}A_7$(ss) is not induced by the melt differentiation.

4. Conclusion

The crystallization experiment was performed for the complete melt with 52.9 mass% CaO and $AR_m = 0.70$. Because the phase composition at ambient temperature was C_3S(ss), C_2S(ss), zoned ferrite and C_3A(ss), the melt-differentiation reaction most probably occurred in accordance with the predicted path. As the crystallization of C_3S(ss), C_2S(ss) and ferrite proceeds during cooling, the coexisting melt would become enriched in the Al_2O_3 component. Immediately after the termination of the crystallization of ferrite, the C_3A(ss) would start to crystallize out of the residual melt. The crystallization of $C_{12}A_7$(ss) was hardly expected because the chemical composition of the finally differentiated melt would lie within the C_3S(ss)–C_2S(ss)–ferrite–C_3A(ss) subsystem.

Acknowledgments

Thanks are due to Mr. T. Bessho, Nagoya Institute of Technology, for technical assistance. This study was supported by a grant from the Japan Cement Association.

References

[1] K. Fukuda, N. Hattori, H. Yoshida, Fractional crystallization of liquid coexisting with α-Ca_2SiO_4 solid solution in $CaO–SiO_2–Al_2O_3–Fe_2O_3$ pseudoquaternary system, J. Am. Ceram. Soc. 86 (2003) 2154–2161.
[2] K. Fukuda, K. Matsunaga, T. Bessho, H. Yoshida, Melt differentiation induced by zonal structure formation of calcium aluminoferrite in a $CaO–SiO_2–Al_2O_3–Fe_2O_3$ pseudoquaternary system, J. Am. Ceram. Soc. 88 (2005) 954–962.
[3] K. Fukuda, T. Iwata, H. Yoshida, Melt differentiation induced by crystallization of cement clinker minerals in a $CaO–SiO_2–Al_2O_3–Fe_2O_3$ pseudoquaternary system, J. Am. Ceram. Soc. 91 (2008) 4093–4100.
[4] M.A. Swayze, A report on studies of the ternary system $CaO–C_5A_3–C_2F$; the quaternary system $CaO–C_5A_3–C_2F–C_2S$; The quaternary system as modified by 5% magnesia, Am. J. Sci. 244 (1946) 1–30.
[5] M. Maultzsch, H. Scholze, Formation of the ferritic clinker phases from the melt, Zem.-Kalk-Gips 26 (1973) 583–587.
[6] K. Fukuda, T. Bessho, K. Matsunaga, H. Yoshida, Chemical zoning of calcium aluminoferrite formed during melt crystallization in $CaO–SiO_2–Al_2O_3–Fe_2O_3$ pseudoquaternary system, Cem. Concr. Res. 34 (2004) 1535–1540.
[7] C. Dong, PowderX: Windows-95-based program for powder x-ray diffraction data processing, J. Appl. Crystallogr. 32 (1999) 838.
[8] K. Fukuda, H. Ando, Determination of the *Pcmn*/*lbm*2 phase boundary at high temperatures in the system $Ca_2Fe_2O_5–Ca_2Al_2O_5$, J. Am. Ceram. Soc. 85 (2002) 1300–1302.
[9] K. Fukuda, S. Inoue, H. Yoshida, Cationic substitution in tricalcium aluminate, Cem. Concr. Res. 33 (2003) 1771–1775.
[10] H.F.W. Taylor, Cement Chemistry, Thomas Telford Publishing, London, U.K., 1997.
[11] F.M. Lea, Application of phase-equilibrium studies on the system $CaO–Al_2O_3–SiO_2–Fe_2O_3$ to cement technology, Cem. Manuf. 8 (1935) 29–49.